

EFFICACY OF MULTIUSER MASSIVE MISO WIRELESS ENERGY TRANSFER UNDER IQI IMBALANCE AND CHANNEL ESTIMATION ERRORS OVER RICIAN FADING

Deepak Mishra and Håkan Johansson

Linköping University, Div. Commun. Syst., Dept. of Electrical Engineering, 58183 Linköping, Sweden

ABSTRACT

We investigate the practical realization of energy beamforming gains in the downlink wireless power transfer from a massive antenna radio frequency (RF) source to multiple single antenna energy harvesting (EH) users. Assuming channel reciprocity for the uplink and downlink channels undergoing Rician fading, we first obtain the least-squares and linear-minimum-mean-square-error channel estimates using the energy-constrained pilot signal transmission from EH users. Due to the usage of low cost hardware at the users and for realizing massive antenna system at the RF source, these estimates are strongly influenced by the transmitter and receiver in-phase-and-quadrature-phase imbalance (IQI). Using these channel estimates, we next derive the harvested power at each user by applying the source transmit precoding that maximizes the sum harvested power among the users. Selected results generated considering practical RF EH system parameters show that IQI and channel estimation errors can lead to about 30% degradation in the sum EH performance.

Index Terms— RF energy harvesting, IQ imbalance, massive MISO, channel estimation, LMMSE, least-squares, beamforming.

1. INTRODUCTION

Massive antenna array at the radio frequency (RF) source can help in realizing the long range wireless power transfer (WPT) to RF energy harvesting (EH) users [1]. Also, if the accurate channel state information (CSI) is available at the transmitter (TX), then it can enable the perpetual operation of low power EH devices in the internet of things (IoT) [2]. However, due to the usage of low cost hardware and low quality RF components for the ubiquitous deployment of EH devices in IoT and for making massive antenna array system economically viable, the performance of these multiple antenna energy sustainable systems is more prone to RF imperfections [3]. Unfortunately, this may result in a significant performance degradation due to the underlying TX and receiver (RX) in-phase-and-quadrature-phase-imbalance (IQI) and its impact on the channel estimation (CE) errors [4]. This work aims at investigating this performance degradation in the energy beamforming gains [5, 6] of practical multiuser (MU) massive multiple-input-single-output (MISO) WPT [1, 2].

1.1. Related Works and Motivation

Recently, in [7] it was shown that due to IQI in MU massive MISO systems, every single antenna RX can be viewed as having two ports, one actual and other virtual, which leads to an inaccurate CE at the multiple antenna TX. Capitalizing on this observation, the impact of IQI on CE and information transfer (IT) was investigated in [4, 8, 9] for the MU massive MISO systems. On one hand, the performance of uplink (UL) massive MISO systems was investigated in [8] and [9] while incorporating the CE and IQI compensation. Whereas, the

authors in [4] studied CE and sum rate limits in downlink (DL) MU massive MISO systems. However, these works [4, 7–9] focusing on IT, did not investigate the impact of IQI and CE errors on the efficacy of massive MISO WPT. Further, only linear-minimum-mean-square-error (LMMSE) based CE was presented in [4, 8, 9] which requires the distribution of channel and noise to be known a priori.

The impact of CE errors on the EH performance of WPT from massive antenna TX to single and multiple users was respectively investigated in [5] and [6]. Different from [4, 8, 9], Rician fading was considered in [5, 6] due to the availability of strong line-of-sight (LoS) component in short range WPT links where TX to RX distance is constrained by low receive energy sensitivity [1, 10] of RF EH devices. *To the best of our knowledge, the joint impact of IQI and CE errors on the optimized sum EH performance of MU massive MISO WPT over Rician channels has not been investigated yet.*

1.2. Key Contributions and Notations

The key contribution of this work is two-fold. (1) Considering the impact of IQI on the RF EH performance degradation for the first time, we derive both the LMMSE and least-squares (LS) based Rician channel estimates for the DL WPT in a MU massive MISO system. (2) Using these estimates we obtain the harvested direct-current (DC) power [11, 12] at each user by applying the TX precoding that maximizes the sum harvested power among the EH users. To corroborate our investigation and quantify the degradation in EH performance, the variation of this sum harvested power under IQI and CE errors with practical WPT system parameters is compared against the maximum value as obtained for perfect CSI with no IQI.

Notations: Vectors and matrices are denoted by boldface lowercase and boldface capital letters, respectively. \mathbf{A}^H , \mathbf{A}^T , \mathbf{A}^* , and \mathbf{A}^{-1} respectively denote the Hermitian transpose, transpose, conjugate, and inverse of matrix \mathbf{A} . $\mathbf{0}_{n \times n}$ and \mathbf{I}_n respectively represent the $n \times n$ zero and identity matrices. With $\text{tr}(\mathbf{A})$ being the trace of matrix \mathbf{A} and $[\mathbf{A}]_{i,k}$ denoting its (i, k) th element, $[\mathbf{D}]_i$ denotes the i th diagonal entry of the diagonal matrix \mathbf{D} . $\|\cdot\|$ and $|\cdot|$ respectively represent the Euclidean norm of a complex vector and the absolute value of a complex scalar. Lastly, with $j = \sqrt{-1}$ and \mathbb{C} denoting the complex number set, $\mathbb{CN}(\boldsymbol{\mu}, \mathbf{C})$ represents the complex Gaussian distribution with mean vector $\boldsymbol{\mu}$ and covariance matrix \mathbf{C} .

2. SYSTEM DESCRIPTION

In this section we first present the system model details along with the adopted wireless channel model. Then we develop the received baseband signal model under both TX and RX IQI.

2.1. Multiuser Massive MISO Channel Model

We consider the MU massive MISO WPT from an N antenna RF source \mathcal{S} to the M single antenna EH users $\mathcal{U} = \{\mathcal{U}_1, \mathcal{U}_2, \dots, \mathcal{U}_M\}$.

This research work is funded by the ELLIIT.

With $N \gg M$, we assume flat quasi-static Rician block fading where the channel impulse response for each communication link remains constant during a coherence interval of τ symbol duration and varies independently across different coherence blocks. \mathcal{S} -to- \mathcal{U}_i channel as represented by an $N \times 1$ vector \mathbf{h}_i is defined below.

$$\mathbf{h}_i = \sqrt{\frac{\beta_i K_i}{K_i + 1}} \mathbf{h}_{d_i} + \sqrt{\frac{\beta_i}{K_i + 1}} \mathbf{h}_{s_i}, \quad \forall i = 1, 2, \dots, M, \quad (1)$$

where $\mathbf{h}_{d_i} \in \mathbb{C}^{N \times 1}$ is a deterministic vector containing the LoS and specular components of the Rician channel \mathbf{h}_i , β_i models the large-scale fading between \mathcal{S} and \mathcal{U}_i which includes both the distance-dependent path loss and shadowing, K_i is the Rician factor denoting the power ratio between the deterministic and scattered components of the \mathcal{S} -to- \mathcal{U}_i channel. On the other hand, $\mathbf{h}_{s_i} \in \mathbb{C}^{N \times 1}$ is a complex Gaussian random vector, with independent and identically distributed zero-mean unit-variance entries, representing the scattered components of the \mathcal{S} -to- \mathcal{U}_i channel.

Thus, $\mathbf{h}_i \sim \mathbb{CN}(\boldsymbol{\mu}_{\mathbf{h}_i}, \mathbf{C}_{\mathbf{h}_i})$, where $\boldsymbol{\mu}_{\mathbf{h}_i} = \sqrt{\frac{\beta_i K_i}{K_i + 1}} \left[\sqrt{\alpha_{i0}} \sqrt{\alpha_{i1}} e^{j\theta_{i1}(\psi_i)} \dots \sqrt{\alpha_{iN-1}} e^{j\theta_{iN-1}(\psi_i)} \right]^T$ and $\mathbf{C}_{\mathbf{h}_i} = \frac{\beta_i}{K_i + 1} \mathbf{I}_N$. Here, α_{i_k} and θ_{i_k} respectively represent the power gain of k th antenna at \mathcal{S} for \mathcal{U}_i and its phase shift with respect to the reference antenna, while ψ_i is the angle of arrival/departure of the specular component at \mathcal{S} from \mathcal{U}_i . With δ representing the inter-antenna separation at \mathcal{S} , $\theta_{i_k}(\psi_i) \triangleq 2\pi k \delta \sin(\psi_i)$, $\forall k = 1, 2, \dots, N - 1$.

Now let us denote the combined \mathcal{S} -to- \mathcal{U} channel with the matrix $\mathbf{H} \triangleq [\mathbf{h}_1 \mathbf{h}_2 \dots \mathbf{h}_M] \in \mathbb{C}^{N \times M}$. In this work, we refer the \mathcal{S} -to- \mathcal{U} channel as DL and the \mathcal{U} -to- \mathcal{S} as UL. Assuming channel reciprocity due to the adoption of widely incorporated time-division duplex (TDD) mode of communication in MU massive MISO systems [4–9], the DL channel coefficients are obtained by estimating them from the UL pilot transmission from the M EH users. We consider that each coherence interval of τ symbol period duration is divided into two subphases, namely, UL CE phase and DL WPT phase. During the CE phase of $M \leq \tau_c \leq \tau$ symbol period duration [2, 4, 6], each \mathcal{U}_i transmits orthogonal pilot signal vector $\mathbf{s}_{p_i} \in \mathbb{C}^{\tau_c \times 1}$ to \mathcal{S} . With p_c denoting the UL CE or training average transmit power of each user \mathcal{U}_i for each symbol period, the combined orthogonal pilot signal matrix can be represented by $\mathbf{S}_p \triangleq [\mathbf{s}_{p_1} \mathbf{s}_{p_2} \dots \mathbf{s}_{p_M}]^T \in \mathbb{C}^{M \times \tau_c}$, which satisfies $\mathbf{S}_p \mathbf{S}_p^H = p_c \tau_c \mathbf{I}_M$. Hence, with $p_c \tau_c$ representing the energy consumption at \mathcal{U} during the CE phase, the resulting received baseband signal $\mathbf{Y} \in \mathbb{C}^{N \times \tau_c}$ at \mathcal{S} without any TX or RX IQI is given by

$$\mathbf{Y} = \mathbf{H} \mathbf{S}_p + \mathbf{W}, \quad (2)$$

where $\mathbf{W} \in \mathbb{C}^{N \times \tau_c}$ is the received complex additive white Gaussian noise (AWGN) matrix with zero mean entries having variance σ_w^2 .

2.2. IQ Imbalance Model

Now we derive the received baseband signal at \mathcal{S} under both TX and RX IQI. The baseband TX IQI in \mathbf{S}_p during the UL transmission from \mathcal{U} can be modeled as follows [3]

$$\mathbf{S}_{p\text{TI}} = \mathbf{T}_{U1} \mathbf{S}_p + \mathbf{T}_{U2} \mathbf{S}_p^*. \quad (3)$$

Here, \mathbf{T}_{U1} and \mathbf{T}_{U2} represent the $M \times M$ diagonal matrices with their i th diagonal entries respectively defined as $[\mathbf{T}_{U1}]_i \triangleq \frac{1}{2} (1 + g_{\mathcal{T}_{U1}} e^{j\phi_{\mathcal{T}_{U1}}})$ and $[\mathbf{T}_{U2}]_i \triangleq \frac{1}{2} (1 - g_{\mathcal{T}_{U2}} e^{j\phi_{\mathcal{T}_{U2}}})$, where $g_{\mathcal{T}_{U1}}$ and $\phi_{\mathcal{T}_{U1}}$ respectively denote the TX amplitude and phase mismatch at the i th user \mathcal{U}_i . Similarly, the baseband RX IQI in \mathbf{Y} at \mathcal{S} during the UL transmission from \mathcal{U} can be modeled as [3]

$$\mathbf{Y}_{\text{RI}} = \mathbf{R}_{S1} \mathbf{Y} + \mathbf{R}_{S2} \mathbf{Y}^*, \quad (4)$$

where \mathbf{R}_{S1} and \mathbf{R}_{S2} represent the $N \times N$ diagonal matrices with their i th diagonal entries respectively defined as $[\mathbf{R}_{S1}]_i \triangleq \frac{1}{2} (1 + g_{\mathcal{R}_{S1}} e^{-j\phi_{\mathcal{R}_{S1}}})$ and $[\mathbf{R}_{S2}]_i \triangleq \frac{1}{2} (1 - g_{\mathcal{R}_{S2}} e^{j\phi_{\mathcal{R}_{S2}}})$, where $g_{\mathcal{R}_{S1}}$ and $\phi_{\mathcal{R}_{S1}}$ respectively denote the RX amplitude and phase mismatch at the i th antenna of \mathcal{S} . Using (3) and (4) in (2), the received UL baseband signal matrix $\mathbf{Y}_{\text{JI}} \in \mathbb{C}^{N \times \tau_c}$ at \mathcal{S} during the CE phase with joint TX and RX IQI can be obtained as

$$\mathbf{Y}_{\text{JI}} = \mathbf{H}_A \mathbf{S}_p + \mathbf{H}_B \mathbf{S}_p^* + \mathbf{W}_{\text{JI}}, \quad (5)$$

where $\mathbf{H}_A \triangleq \mathbf{R}_{S1} \mathbf{H} \mathbf{T}_{U1} + \mathbf{R}_{S2} \mathbf{H}^* \mathbf{T}_{U2}^*$, $\mathbf{H}_B \triangleq \mathbf{R}_{S1} \mathbf{H} \mathbf{T}_{U2} + \mathbf{R}_{S2} \mathbf{H}^* \mathbf{T}_{U1}^*$, and $\mathbf{W}_{\text{JI}} \triangleq \mathbf{R}_{S1} \mathbf{W} + \mathbf{R}_{S2} \mathbf{W}^*$. It is worth noting that due to the usage of narrow band signals for DL WPT [1, 2, 10] and UL pilot signal transmission [4, 8], we have considered the frequency-independent IQI model [3]. Further, due to the limited availability of feedback or training signals at \mathcal{S} from the energy-constrained users \mathcal{U} , we assume that \mathcal{S} does not compensate for IQI and treats $\mathbf{H}_B \mathbf{S}_p^*$ and \mathbf{W}_{JI} in (5) as the interference and scaled noise, respectively, which stem from joint TX-RX IQI. As we consider IQI in both UL CE and DL WPT, instead of TX or RX IQI, now onwards we denote IQI at \mathcal{S} and \mathcal{U} as \mathcal{S} -IQI and \mathcal{U} -IQI, respectively.

3. UPLINK CHANNEL ESTIMATION UNDER TX-RX IQI

Here we present the LS and LMMSE channel estimates for the effective channel \mathbf{H}_A as defined in (5) for the joint \mathcal{S} - \mathcal{U} -IQI. In order to have sufficient time for WPT to enable efficient RF EH at \mathcal{U} , we set $\tau_c = M$, allocating the minimum time required for CE phase [4, 6].

3.1. LS based Channel Estimate

The LS based CE can be used when the distribution of the channel and noise are not known a priori. From (5), the LS estimate $\hat{\mathbf{H}}_{A_L} \in \mathbb{C}^{N \times M}$ for the effective channel \mathbf{H}_A under IQI is given by [13]

$$\hat{\mathbf{H}}_{A_L} = \mathbf{Y}_{\text{JI}} \mathbf{S}_p^H \left(\mathbf{S}_p \mathbf{S}_p^H \right)^{-1} = \mathbf{Y}_{\text{JI}} \mathbf{S}_p^H (p_c \tau_c)^{-1}, \quad (6)$$

where with $\mathbf{H}_d \triangleq [\mathbf{h}_{d_1} \mathbf{h}_{d_2} \dots \mathbf{h}_{d_M}]$ representing the combined deterministic components of the channel \mathbf{H} , the mean of $\hat{\mathbf{H}}_{A_L}$ is given by $\boldsymbol{\mu}_{\hat{\mathbf{H}}_{A_L}} = \mathbf{R}_{S1} \mathbf{H}_d \mathbf{T}_{U1} + \mathbf{R}_{S2} \mathbf{H}_d^* \mathbf{T}_{U2}^* + \left[\mathbf{R}_{S1} \mathbf{H}_d \mathbf{T}_{U2} + \mathbf{R}_{S2} \mathbf{H}_d^* \mathbf{T}_{U1}^* \right] \frac{\mathbf{S}_p^* \mathbf{S}_p^H}{p_c \tau_c}$ and variance $[\mathbf{C}_{\hat{\mathbf{H}}_{A_L}}]_{ik}$ of the element in i th row and k th column of $\hat{\mathbf{H}}_{A_L}$ for the real-valued \mathbf{S}_p (special case) is

$$[\mathbf{C}_{\hat{\mathbf{H}}_{A_L}}]_{ik} = \frac{\beta_k}{K_k + 1} (|[\mathbf{R}_{S1}]_i|^2 + |[\mathbf{R}_{S2}]_i|^2) + \frac{[\mathbf{C}_{\mathbf{W}_{\text{JI}}}]_i}{p_c \tau_c}, \quad (7)$$

where $\mathbf{C}_{\mathbf{W}_{\text{JI}}} = \sigma_w^2 (|\mathbf{R}_{S1}|^2 + |\mathbf{R}_{S2}|^2)$ represents the covariance matrix of \mathbf{W}_{JI} as defined in (5). The detailed proof for obtaining (7) has been omitted here due to the limited space. Also, it may be noted that as suggested in [14], a special structured \mathbf{S}_p can be considered for reducing the impact of IQI on LS based CE. However, this requires a novel pilot matrix design investigation that considers the limited energy-constraint and feedback availability from EH \mathcal{U} .

3.2. LMMSE based Channel Estimate

LMMSE can provide a much more accurate CE if the distribution of the channel and noise are known a priori [5]. Using (5), the LMMSE estimate $\hat{\mathbf{H}}_{A_M} \in \mathbb{C}^{N \times M}$ for \mathbf{H}_A can be obtained as [13]

$$\hat{\mathbf{H}}_{A_M} = \boldsymbol{\mu}_{\mathbf{H}_A} + \mathbf{C}_{\mathbf{H}_A, \mathbf{Y}_{\text{JI}}} (\mathbf{C}_{\mathbf{Y}_{\text{JI}}})^{-1} (\mathbf{Y}_{\text{JI}} - \boldsymbol{\mu}_{\mathbf{Y}_{\text{JI}}}), \quad (8)$$

where $\boldsymbol{\mu}_{\mathbf{H}_A}$ and $\boldsymbol{\mu}_{\mathbf{Y}_{JI}}$ represent the respective means of \mathbf{H}_A and \mathbf{Y}_{JI} , with $\mathbf{C}_{\mathbf{H}_A, \mathbf{Y}_{JI}}$ representing the cross-covariance matrix of \mathbf{H}_A and \mathbf{Y}_{JI} , and $\mathbf{C}_{\mathbf{Y}_{JI}}$ denoting the covariance matrix of \mathbf{Y}_{JI} . In (8) matrix vectorization is used for applying the canonical form of vector estimation [13], and mean of $\hat{\mathbf{H}}_{A_M}$ is given by $\boldsymbol{\mu}_{\hat{\mathbf{H}}_{A_M}} = \boldsymbol{\mu}_{\mathbf{H}_A} = (\mathbf{R}_{S1} \mathbf{H}_d \mathbf{T}_{U1} + \mathbf{R}_{S2} \mathbf{H}_d^* \mathbf{T}_{U2}^*)$ with the variance $[\mathbf{C}_{\hat{\mathbf{H}}_{A_M}}]_{ik}$ of the (i, k) th element of $\hat{\mathbf{H}}_{A_M} \forall (1 \leq i \leq N, 1 \leq k \leq M)$ defined below

$$[\mathbf{C}_{\hat{\mathbf{H}}_{A_M}}]_{ik} = \frac{\left(\frac{\beta_k}{K_k+1}\right)^2 \|\mathbf{R}_{S1}\|_i^4}{\left(\frac{\beta_k}{K_k+1} + \frac{\sigma_w^2}{p_c \tau_c}\right) (\|\mathbf{R}_{S1}\|_i^2 + \|\mathbf{R}_{S2}\|_i^2)}. \quad (9)$$

Intermediate steps in the derivation of (9) under real-valued \mathbf{S}_p assumption have not been included. However, it can be obtained using the similar steps as outlined in proofs for Propositions 1 and 2 in [4].

4. DOWNLINK WIRELESS RF POWER TRANSFER

In this section we first present the optimal TX precoding that maximizes the sum harvested power among the users with perfect CSI availability at \mathcal{S} and no IQI. Later, we extend this result to obtain the sum harvested power for both LS and LMMSE estimates with IQI.

4.1. Ideal Scenario: Perfect CSI with No IQI

The received RF energy signal $\mathbf{y}_e \in \mathbb{C}^{M \times 1}$ at the users \mathcal{U} due to the DL WPT with perfect CSI and no IQI can be defined as

$$\mathbf{y}_e = \mathbf{H}^T \mathbf{x} + \mathbf{w}_u, \quad (10)$$

where $\mathbf{x} \in \mathbb{C}^{N \times 1}$, satisfying $\text{tr}(\mathbf{x} \mathbf{x}^H) = p_e$, is the TX precoding vector with p_e being the transmit power for the DL WPT and $\mathbf{w}_u \sim \mathcal{CN}(\mathbf{0}_{M \times 1}, \sigma_w^2 \mathbf{I}_M)$ is the received AWGN at \mathcal{U} . Hence, ignoring the negligible harvested power from the noise signal \mathbf{w}_u due to low receive energy sensitivity [2, 10] and denoting nonlinear RF-to-DC rectification efficiency [11, 12] at each EH user by η , the sum harvested DC power during each of the remaining $\tau - \tau_c$ symbol period duration is given by $P_H = \eta \text{tr}(\mathbf{y}_e \mathbf{y}_e^H) = \eta \text{tr}(\mathbf{H}^T \mathbf{x} \mathbf{x}^H \mathbf{H}^*)$. To maximize this sum harvested DC power P_H among M EH users, with the availability of perfect CSI at \mathcal{S} with no IQI, the optimal TX precoding can be obtained as [15]

$$\mathbf{x}_{\text{opt}} = \sqrt{p_e} \mathbf{v}_{\max}(\mathbf{H}^* \mathbf{H}^T), \quad (11)$$

where $\mathbf{v}_{\max}(\mathbf{H}^* \mathbf{H}^T) \in \mathbb{C}^{N \times 1}$ represents the eigenvector corresponding to the largest eigenvalue $\lambda_{\max}(\mathbf{H}^* \mathbf{H}^T)$ of the matrix $\mathbf{H}^* \mathbf{H}^T$. With $\|\mathbf{v}_{\max}(\mathbf{H}^* \mathbf{H}^T)\| = 1$, the maximum sum harvested DC power $P_{H_{\text{opt}}}$ under this ideal scenario can be obtained as

$$P_{H_{\text{opt}}} = \eta p_e \lambda_{\max}(\mathbf{H}^* \mathbf{H}^T). \quad (12)$$

This maximum sum harvested power $P_{H_{\text{opt}}}$ is used as a benchmark to compare the performance degradation due to IQI and CE errors.

4.2. Under IQI and Channel Estimation Errors

Using (10), the received energy signal $\mathbf{y}_{eTI} \in \mathbb{C}^{M \times 1}$ at users \mathcal{U} during the DL WPT under the TX IQI in DL (i.e., \mathcal{S} -IQI) is given by

$$\mathbf{y}_{eTI} = \mathbf{H}^T (\mathbf{T}_{S1} \mathbf{x} + \mathbf{T}_{S2} \mathbf{x}^*) + \mathbf{w}_u \quad (13)$$

where \mathbf{T}_{S1} and \mathbf{T}_{S2} represent $N \times N$ diagonal matrices with $g_{\mathbf{T}_{S1}i}$ and $\phi_{\mathbf{T}_{S1}i}$ in their i th diagonal entries $[\mathbf{T}_{S1}]_i \triangleq \frac{1}{2} (1 + g_{\mathbf{T}_{S1}i} e^{j\phi_{\mathbf{T}_{S1}i}})$

and $[\mathbf{T}_{S2}]_i \triangleq \frac{1}{2} (1 - g_{\mathbf{T}_{S1}i} e^{j\phi_{\mathbf{T}_{S1}i}})$ respectively denote the TX amplitude and phase mismatch at the i th antenna at \mathcal{S} . It is worth noting that the DL WPT does not suffer from the RX IQI in DL (or \mathcal{U} -IQI) because RF EH does not require the RF to baseband conversion [2, 10] that may suffer IQI. Rather, the harvested DC power is directly obtained from the received RF power after the RF-to-DC conversion by the RF EH circuit [2, 10–12] available at the EH users. Thus, we can observe that the \mathcal{U} -IQI only affects the UL CE phase, whereas the \mathcal{S} -IQI affects both UL CE and DL WPT phases. Thus, as also verified later by the numerical results in Section 5, \mathcal{S} -IQI leads to more significant degradation as compared to \mathcal{U} -IQI.

Using the channel estimate, LS $\hat{\mathbf{H}}_{A_L}$ or LMMSE $\hat{\mathbf{H}}_{A_M}$, along with (11), the TX precoding under IQI and CE errors is given by

$$\mathbf{x}_{\hat{\mathbf{H}}_{A_E}} = \sqrt{p_e} \mathbf{v}_{\max}(\hat{\mathbf{H}}_{A_E}^* \hat{\mathbf{H}}_{A_E}^T), \quad \forall E = \{L, M\}, \quad (14)$$

and the corresponding sum harvested DC power $P_{\hat{\mathbf{H}}_{A_E}}$ is derived as

$$P_{\hat{\mathbf{H}}_{A_E}} = \eta \text{tr}(\mathbf{H}^T (\mathbf{T}_{S1} \mathbf{x}_{\hat{\mathbf{H}}_{A_E}} + \mathbf{T}_{S2} \mathbf{x}_{\hat{\mathbf{H}}_{A_E}}^*) \times (\mathbf{x}_{\hat{\mathbf{H}}_{A_E}}^H \mathbf{T}_{S1}^H + \mathbf{x}_{\hat{\mathbf{H}}_{A_E}}^T \mathbf{T}_{S2}^H) \mathbf{H}^*), \quad \forall E = \{L, M\}. \quad (15)$$

Following the definition in (12), it can be observed that $P_{\hat{\mathbf{H}}_{A_E}} \leq P_{H_{\text{opt}}}$, $\forall E = \{L, M\}$, and we can define the percentage RF EH performance degradation by $\Delta_{P_{A_E}} \triangleq (1 - P_{\hat{\mathbf{H}}_{A_E}} / P_{H_{\text{opt}}}) \times 100\%$, $\forall E = \{L, M\}$. To obtain the RF EH performance degradation due to \mathcal{S} -IQI only, we need to set $\mathbf{T}_{U1} = \mathbf{I}_M$ and $\mathbf{T}_{U2} = \mathbf{0}_{M \times M}$ in (15). Similarly, for investigating the \mathcal{U} -IQI alone, substitute $\mathbf{R}_{S1} = \mathbf{T}_{S1} = \mathbf{I}_N$ and $\mathbf{R}_{S2} = \mathbf{T}_{S2} = \mathbf{0}_{N \times N}$ in (15). Next we compare this degradation $\Delta_{P_{A_E}}$ in $P_{H_{\text{opt}}}$ due to CE errors alone and along with \mathcal{U} -IQI, \mathcal{S} -IQI, and joint- \mathcal{S} - \mathcal{U} -IQI (called joint-IQI).

5. NUMERICAL PERFORMANCE EVALUATION

Here, we evaluate the sum harvested DC power among the EH users under IQI and CE errors. Unless otherwise stated, we have used $N = 40$, $M = 12$, $\tau = 120$ and $\tau_c = 12$, each having symbol duration of $8.33 \mu\text{s}$, $p_e = 30 \text{dBm}$, $p_c = -40 \text{dBm}$, $\sigma_w^2 = 10^{-16}$ Joule, $g_{\mathbf{T}_{U1}i} = g_{\mathbf{T}_{S1}i} = g_{\mathbf{R}_{S1}i} = 1 - 0.15\xi$, $\phi_{\mathbf{T}_{U1}i} = \phi_{\mathbf{T}_{S1}i} = \phi_{\mathbf{R}_{S1}i} = 15^\circ \xi$, with $\xi = 1 \forall i$, $\delta = \frac{3 \times 10^8}{2f}$, $K_i = 2$, $\alpha_i = 1$ and $\beta_i = \varpi d_i^{-\rho}$, $\forall i$, where $\varpi = \left(\frac{3 \times 10^8}{4\pi f}\right)^2$ being the average channel attenuation at unit reference distance with $f = 915 \text{MHz}$ [12] being TX frequency, d_i is \mathcal{S} to \mathcal{U}_i distance, and $\rho = 2.5$ is the path loss exponent. For incorporating the practical nonlinear RF-to-DC conversion operation at \mathcal{U} , η is modeled using [11, equation (6)] for the commercially available RF EH circuit from Powercast [12]. The M users have been placed uniformly over a square field with length $L = 7 \text{m}$ and \mathcal{S} placed at its center. For the average sum harvested power results we used 10^3 independent channel realizations and complex pilot \mathbf{S}_p .

First via Fig. 1 we investigate the performance of the sum harvested power among users for the ‘ideal’ scenario (perfect CSI with no IQI) against the practical scenarios which include: (a) only CE errors with no IQI (called ‘No IQI’), (b) \mathcal{U} -IQI with CE errors, (c) \mathcal{S} -IQI with CE errors, and (d) the joint- \mathcal{S} - \mathcal{U} -IQI with CE errors. For each case, both LS and LMMSE based CE results are plotted with varying N . It is observed that the \mathcal{U} -IQI alone does not have a significant impact on the sum EH performance. Whereas, for both LS and LMMSE based CE, the \mathcal{S} -IQI has a more significant impact and it closely follows the degradation caused by the joint- \mathcal{S} - \mathcal{U} -IQI. The

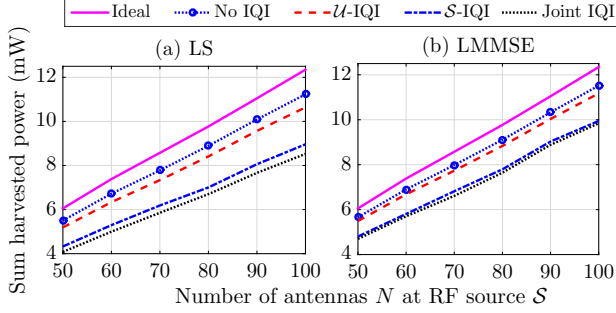


Fig. 1. Variation with increasing antennas N at source.

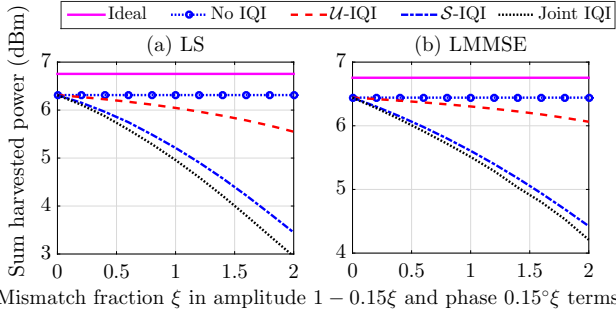


Fig. 2. Variation with increasing mismatch fraction ξ in the amplitude and phase parameters representing the TX and RX IQI.

main reason behind this outcome, as also explained in Section 4.2, is that S -IQI affects both UL CE and DL WPT. Further, LMMSE requiring additional prior information can provide a relatively enhanced EH performance as compared to LS based CE. Another key observation from Fig. 1 is that the absolute degradation in sum EH performance gets more enhanced with increasing antennas N at S .

Next we investigate the impact of increased mismatch ξ in the amplitude and phase terms modeling the IQI. In particular, by plotting the variation of ξ from 0 to 2 in Fig. 2, it implies that the amplitude mismatch ($1 - 0.15\xi$) gets enhanced from 1 to 0.7 (30% decrease) and the phase mismatch ($15^\circ\xi$) increases from 0° to 30° . We observe that degradation in sum EH performance gets enhanced with increased mismatch fraction ξ for each IQI for both LS and LMMSE CEs. This degradation is more prominent for IQI in LS based CE. As ξ increases from 0 to 2, leading to 30% amplitude mismatch and 30° phase mismatch, it results in about 54% and 38% decrease in sum EH performance due to joint IQI as compared to that achieved respectively by the LS and LMMSE based CE with no IQI.

Now, we consider the impact of improved UL CE due to the increased transmit power p_c . As shown in Fig. 3, with increased p_c , the degradation in the sum EH performance decreases due to a more accurate CE. In fact, for $p_c > -30$ dBm, the performance of both LS and LMMSE CE, with and without U -IQI, converges to that of the ideal scenario. However, with S -IQI and joint IQI, this degradation cannot be reduced to zero. This result is in accordance to a similar recent observation of [4] for data communication over Rayleigh channels. Thus, S -IQI is a much more bigger threat in realizing the full energy beamforming gains even with very high quality CE. We would also like to add that, as in practice the value of p_c at EH users is very low, it is very difficult to totally eliminate the CE errors.

Lastly, in Fig. 4, we conduct a sum EH performance degradation $\Delta_{P_{A_E}}$ comparison study among the four considered practical scenarios for varying critical system parameters N , ξ , and p_c

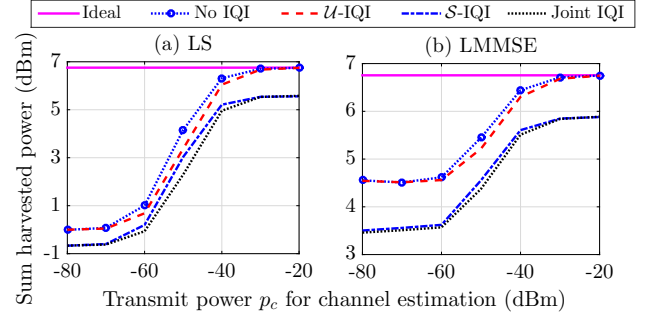


Fig. 3. Impact of increased TX power p_c during CE phase.

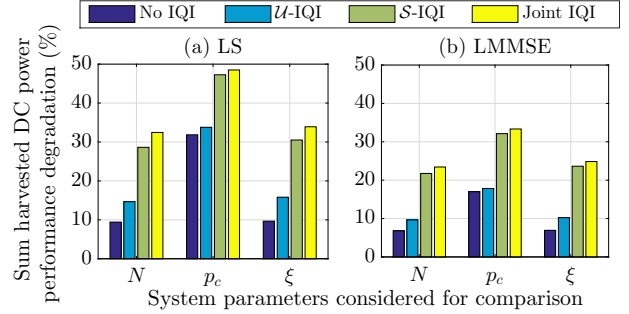


Fig. 4. Comparing percentage degradation in sum EH performance.

(cf. Figs. 1, 2, 3). We observe that the average degradation for no IQI, U -IQI, S -IQI, and joint IQI over the ideal scenario is about 10.25%, 12.58%, 25.84%, and 27.21% for the LMMSE based CE. Whereas it is much higher, i.e., 16.98%, 21.42%, 35.47%, and 38.29%, respectively, for the LS based CE. Hence, we note that the IQI and CE errors can lead to about 30% degradation in the achievable sum harvested power as realized by the ideal energy beamforming gains. Here, more than 18% degradation due to IQI alone signifies that it plays a more prominent role in WPT performance degradation than the CE errors alone.

6. CONCLUDING REMARKS

This paper investigated the practical feasibility of the energy beamforming gains achieved due to MU massive MISO WPT under IQI and CE errors over Rician fading. Both LS and LMMSE estimates were obtained under the joint TX and RX IQI. Using these derived estimates, the sum EH performance was compared against the ideal scenario with optimal TX precoding for perfect CSI availability and no IQI. It was observed that the S -IQI, due to the usage of low quality RF components for realizing massive antenna array gain, can significantly degrade the achievable EH performance. This degradation gets further enhanced with increasing number of antennas N at S . As compared to LS, LMMSE based CE provides a much better performance and is relatively less prone to IQI. Further, we notice that U -IQI for both LS and LMMSE CEs can be mitigated by using high TX power p_c during the UL CE phase. However, this is not practically feasible in low power EH users scenario. Hence, we conclude that IQI can result in much higher EH performance degradation than the CE errors alone and there is a need for the novel green designs for channel and IQI parameter estimation to realize the maximum achievable energy beamforming gains. In future, we would like to investigate the optimal TX precoding design and TX-RX resource allocation to maximize EH performance under IQI and CE errors.

7. REFERENCES

- [1] A. Yazdan, J. Park, S. Park, T. A. Khan, and R. W. Heath, "Energy-efficient massive MIMO: Wireless-powered communication, multiuser MIMO with hybrid precoding, and cloud radio access network with variable-resolution ADCs," *IEEE Microw. Mag.*, vol. 18, no. 5, pp. 18–30, July 2017.
- [2] Y. Zeng, B. Clerckx, and R. Zhang, "Communications and signals design for wireless power transmission," *IEEE Trans. Commun.*, vol. 65, no. 5, pp. 2264–2290, May 2017.
- [3] T. Schenk, *RF Imperfections in High-Rate Wireless Systems: Impact and Digital Compensation*, Dordrecht, The Netherlands: Springer, 2008.
- [4] N. Kolomvakis, M. Coldrey, T. Eriksson, and M. Viberg, "Massive MIMO systems with IQ imbalance: Channel estimation and sum rate limits," *IEEE Trans. Commun.*, vol. 65, no. 6, pp. 2382–2396, June 2017.
- [5] S. Kashyap, E. Björnson, and E. G. Larsson, "On the feasibility of wireless energy transfer using massive antenna arrays," *IEEE Trans. Wireless Commun.*, vol. 15, no. 5, pp. 3466–3480, May 2016.
- [6] Y. Zeng and R. Zhang, "Optimized training design for wireless energy transfer," *IEEE Trans. Commun.*, vol. 63, no. 2, pp. 536–550, Feb 2015.
- [7] S. Wang and L. Zhang, "Signal processing in massive MIMO with IQ imbalances and low-resolution ADCs," *IEEE Trans. Wireless Commun.*, vol. 15, no. 12, pp. 8298–8312, Dec. 2016.
- [8] Y. Xiong, N. Wei, Z. Zhang, B. Li, and Y. Chen, "Channel estimation and IQ imbalance compensation for uplink massive MIMO systems with low-resolution ADCs," *IEEE Access*, vol. 5, pp. 6372–6388, Apr. 2017.
- [9] S. Zarei, W. H. Gerstacker, J. Aulin, and R. Schober, "I/Q imbalance aware widely-linear receiver for uplink multi-cell massive MIMO systems: Design and sum rate analysis," *IEEE Trans. Wireless Commun.*, vol. 15, no. 5, pp. 3393–3408, May 2016.
- [10] D. Mishra, S. De, S. Jana, S. Basagni, K. Chowdhury, and W. Heinzelman, "Smart RF energy harvesting communications: Challenges and opportunities," *IEEE Commun. Mag.*, vol. 53, no. 4, pp. 70–78, Apr. 2015.
- [11] D. Mishra and S. De, "Utility maximization models for two-hop energy relaying in practical RF harvesting networks," in *Proc. IEEE ICC*, Paris, France, May 2017, pp. 41–46.
- [12] "Powercast datasheet – P1110B Powerharvester receiver," <http://www.powercastco.com/documentation/>, accessed Oct. 23, 2017.
- [13] S. M. Kay, *Fundamentals of Statistical Signal processing: Estimation Theory*, vol. 1, Upper Saddle River, NJ: Prentice Hall, 1993.
- [14] S. Narayanan, B. Narasimhan, and N. Al-Dhahir, "Training sequence design for joint channel and I/Q imbalance parameter estimation in mobile SC-FDE transceivers," in *Proc. IEEE ICASSP*, Dallas, TX, USA, Mar. 2010, pp. 3186–3189.
- [15] H. Son and B. Clerckx, "Joint beamforming design for multi-user wireless information and power transfer," *IEEE Trans. Wireless Commun.*, vol. 13, no. 11, pp. 6397–6409, Nov 2014.